DESIGN AND OPERATION OF A CURRENT MONITOR UNDER HEAVY HEAT LOAD

P. A. Duperrex, P. Baumann, S. Joray, D. Kiselev, Y. Lee, U. Müller,
Paul Scherrer Institut, 5232 Villigen PSI, Switzerland

Abstract

For high intensity beam operation (3 mA, 1.8 MW) in the PSI 590 MeV 50 MHz cyclotron, a new current monitor for proton beams has been built. This monitor uses a re-entrant cavity tuned at the 2nd RF harmonic. Compared to the current monitors already in operation, the design has improved cooling. The circuit resonance has been optimized in the laboratory to minimize the gain drift due to temperature changes. Energy deposition simulations and thermal analysis were performed to estimate the cooling efficiency, and preliminary results indicate that the temperature rise of the resonator corresponds to values predicted with MARS. Anomalous gain drift is nevertheless observed even with an active cooling system. A drift compensation scheme using a pilot signal 600 kHz off the designed resonator frequency is being presently tested and the preliminary results are encouraging.

INTRODUCTION

A new proton beam current monitor called "MHC5" has been installed in the PSI 590 MeV proton cyclotron. The current monitor is located approximately 8 m behind a 4 cm thick graphite target used for muon and pion production. As a consequence, the monitor is exposed to scattered particles and their secondaries from this target. The resulting thermal load is the main concern for this monitor. This problem will be even acuter for future high intensity beam operation (3 mA, 1.8 MW). Thus the main improvements of the new monitor were an active water cooling system and a surface blackening to improve the radiation cooling.

MAIN FEATURES

Measurement Principle

The current monitor consists of a TM01-mode coaxial resonator, coaxially symmetric with the round proton beam pipe. The resonator is modelled as a quarter-wave transmission line, the open-end gap in the beam pipe couples some of the wall current into the resonator. The cavity is tuned at 101.26 MHz, the 2nd harmonic of the proton beam pulse frequency. This frequency is used because of the better signal-to-noise ratio, the RF noise components from the generator being mainly at the odd harmonics. No significant shape dependency of the 2nd harmonic amplitude for relative small beam pulses is expected [1]. The oscillating magnetic field in the resonator is used to measure the beam current.

Resonance Condition

For a given resonant frequency, using an external capacitor shunt reduces the physical length of the resonator. The corresponding resonance condition is given by:

$$\tan\left(\frac{2\pi L}{\lambda_m}\right) = \frac{\lambda_m}{2\pi c C Z_o}$$

with L the resonator length, C the capacitor shunt, Z_o the characteristic impedance of the transmission line, and λ_m the resonant wavelength.

Mechanical Design

The monitor is made of aluminium (anticorodal 110), with a 10µm coating layer of silver to improve the electrical conductivity. Compared to the monitors already into operation, the thermal coupling conductance was increased to improve the efficiency of the active water cooling. The monitor itself being in vacuum, the external surfaces have been chemically blackened to increase the emissivity of the monitor to provide an additional cooling. Four type K thermocouples monitor the resonator temperature.

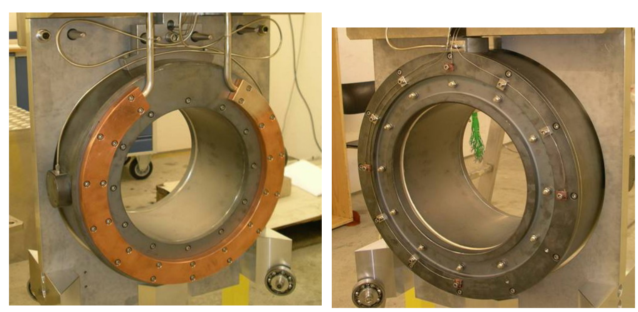

Figure 1: The new current monitor, showing the water cooling circuitry at the beam entry side (left). The four thermocouples are installed on the beam exit side (right).

Temperature Drift Compensation

Effect of temperature changes on the resonant frequency has been measured on a laboratory test bench before the installation of the monitor. External resonant circuits have been added to compensate the temperature drifts. Gain drifts smaller than 0.3dB were measured for the expected temperature variations during beam operation (30 to 70 ^{o}C).

POWER DEPOSITION

To predict the thermal load, the proton deposition rate in the current monitor MHC5 was simulated, using Monte Carlo methods with the MCNPX [2] and MARS [3] programs. In MCNPX, the effect of the magnetic quadrupoles QHG 21 & 22 located between the target and the current monitor cannot be taken into account due to the lack of magnetic module. In MARS, the quadrupole induced beam deflection is taken into account. The MCNPX and the MARS calculations respectively predict 562 W and 345 W energy deposition rate for 3 mA proton beam current. In MCNPX, the Coulomb scattering at the meson target is observed to be stronger, which causes more widely scattered beam thereafter, giving the higher energy deposition rate. In MARS, the beam is more focused due to the presence of quadrupole effect, and the current monitor is less exposed to scattered particle shower.

THERMAL ANALYSIS

Simulation Tools

The applied simulation methods for the thermal analysis include the coupled flow and heat simulations based on second order accurate finite volume scheme and the Monte Carlo simulations for particle transport. The coupled flow and heat simulations have been performed by the multiphysics commercial tool CFDACE+ [4]. For calculation of the heat exchange rate between MHC5 and water, the shear stress transport (SST) $k-\omega$ turbulence model [5] has been used. The mesh in the boundary layer region was refined until the desired value of the wall function is achieved.

Water Cooling Efficiency

For the laboratory test, the monitor MHC5 was thermally isolated and first heated by circulating 80 ^{o}C water through the cooling circuitry. As the monitor reached a thermally stable condition, the monitor was then suddenly cooled down using 30 ^{o}C water. The monitor temperature was observed to decrease exponentially in time during this cooling phase. The corresponding time constant was measured for different water speeds and then compared with the simulation results (Fig. 2). The time constants agree well within the 10 % error for water speeds larger than 0.5 m/s. There is relatively large disagreement in values, for the water velocities below 0.25 m/s. One reason is that the simulation setting uses the turbulence module which might describe the laminar flow region with low water speed inaccurately. Another reason is that there have been more uncertainties in accurately controlling the water velocity for small mass flux.

For reference, the transition from laminar to turbulent flow is expected to occur inside the 10 mm diameter water pipe at around 0.25 m/s. Then, the fully developed turbulent internal flow is formed at a water speed around 0.4 m/s (or Reynolds number 4x10^{3}, see Ref. [6]). Once the turbulence is fully developed, the improvement of the cooling efficiency with increasing water inlet speed is marginal. This phenomenon is well reproduced by the simulation and the measurement.

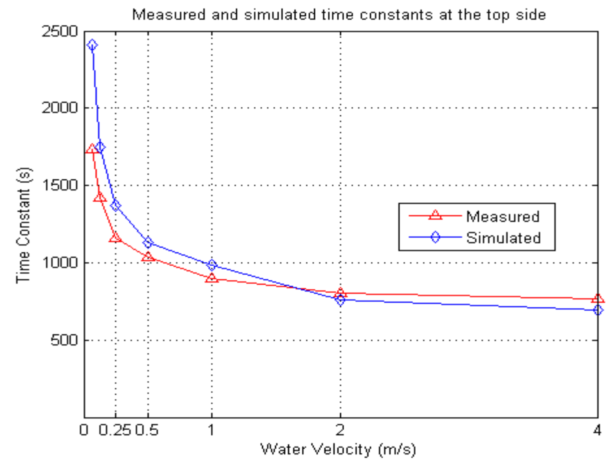

Figure 2: Comparison between measured and simulated time constants at the upper thermocouple location.

Based on these cooling efficiency tests, a speed of 2 m/s was chosen for the water inlet flow. Larger speeds would just accelerate the wearing out of the tube wall without improving the cooling.

Predicted Operating Temperature

For the prediction of the operating temperature of MHC5, a coupled flow and thermal simulation for the energy deposition rate given by MCNPX was performed.

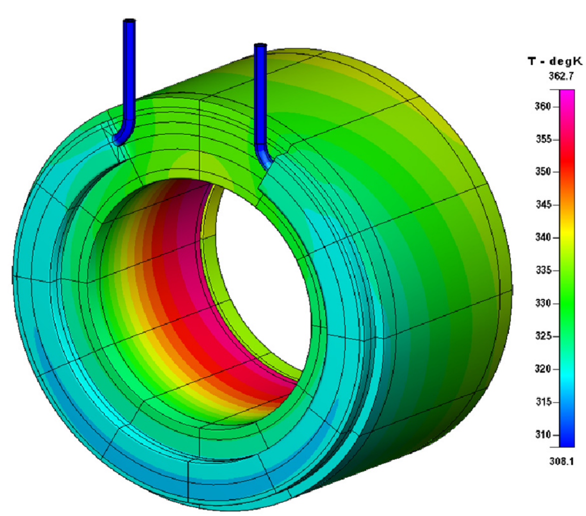

Figure 3: The simulated temperature profile of MHC5 for the proton beam current 3 mA. The temperatures range from 308°K to 363°K.

Figure 4 shows the simulated temperature distribution for a proton beam current 3 mA, with the peak temperature being 90 ^{o}C. For the energy deposition input from MARS, the peak temperature is simulated to be below 70 ^{o}C.

Comparison with Experiment

For the present operating beam current of 2 mA and for a inlet cooling water temperature of 38 ^{o}C, the MARS thermal simulation predicts a temperature of 48 to 49 ^{o}C at the upper PT100 sensor location. This is in excellent agreement with experimentally observed temperature (also 48 to 49 ^{o}C) for a 2 m/s cooling water speed. Thus, MARS delivers a realistic estimate of the power deposition.

PRELIMINARY RESULTS

Measurements of the beam current showed however significant and unexpected drifts for large currents (>1 mA). The drifts are clearly visible when the MHC5 current measurement is compared with a standard current monitor (MHC6) on the same beam line (Fig. 4). After each short beam interruption, MHC5 measurement drifts can be observed whereas MHC6 measurements remain stable. The temperature variations during these measurements were smaller than 5 ^{o}C and they could not account for the observed 10% current measurement drift. Transfer function measurements were thus performed during beam operation and the results clearly show changes larger than those observed during the bench tests.

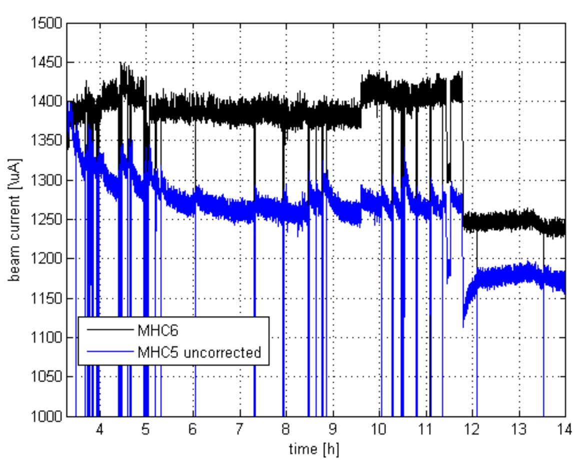

Figure 4: Time evolution of the beam current as measured with standard monitor (MHC6) and with the new monitor (MHC5). MHC5 drifts are clearly visible.

The use of a pilot signal (test signal 600 kHz off the cyclotron RF frequency) to monitor these drifts and to provide a calibration has been investigated. An off-line analysis using MATLAB shows that the pilot signal may indeed compensate the observed drift (Fig. 5) at least during stable beam operation (i.e. no long beam interruptions).

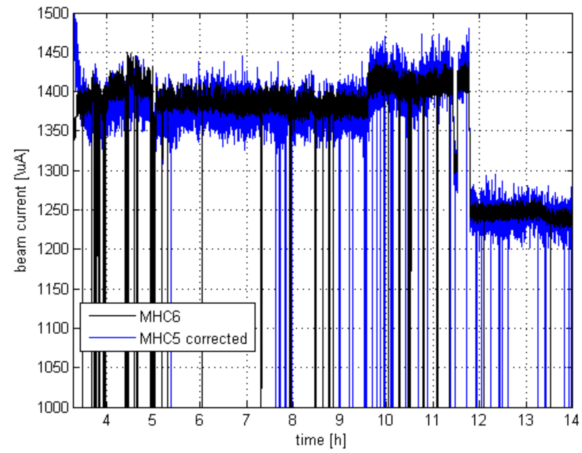

Figure 5: Time evolution of the MHC6 and of the corrected MHC5. The drifts could be compensated by using a pilot signal.

CONCLUSION

The preliminary measurements indicate that temperature measurements are in agreement with power deposition simulations when the magnetic field effects are taken into account (MARS). The beam current measurement drifts are larger than expected and remain for the moment unexplained. Correction schemes using a pilot signal are under investigation and the preliminary results are positive.

REFERENCES

[1] R. Reimann, M. Rüede, “Strommonitor für die Messung eines gepulsten Ionenstrahls”, Nucl. Instr. Meth. 129 (1975) 53.
[2] D.B. Pelowitz, ed., “MCNPX User’s Manual,” Version 2.5.0, LA-CP-05-0369
[3] N.V. Mokhov, C.C. James, “The MARS Code System User’s Guide,” Version 15, 2007.
[4] CFD-ACE+, http://www.esi-group.com.
[5] F.R. Menter, “Zonal Two Equation $k-\omega$ Turbulence Models for Aerodynamic Flows”, AIAA Paper 93-2906.
[6] J. P. Holman, “Heat Transfer,” McGraw-Hill, 2002.